



Experimental and Preliminary Clinical Study of Real-Time Registration in Liver Tumors During Respiratory Motion Based on a Multimodality Image Navigation System

Technology in Cancer Research & Treatment
 Volume 18: 1-9
 © The Author(s) 2019
 Article reuse guidelines:
sagepub.com/journals-permissions
 DOI: 10.1177/1533033819857767
journals.sagepub.com/home/tct


Chao Ren, MD¹ , Shi-rong Liu, MD², Wen-bo Wu, MS³, Xiao-ling Yu, MD¹, Zhi-gang Cheng, MD¹, Fang-yi Liu, MD¹, and Ping Liang, MD¹

Abstract

Purpose: To develop a fusion imaging system that combines ultrasound and computed tomography for real-time tumor tracking and to validate the accuracy of performing registration via this approach during a specific breathing phase. **Materials and Methods:** The initial part of the experimental study was performed using iodized oil injection in pig livers and was focused on determining the accuracy of registration. Eight points (A1-4 and B1-4) at different positions and with different target sizes were selected as target points. During respiratory motion, we used our self-designed system to perform the procedure either with (experimental group, E) or without (control group, C) the respiratory monitoring module. The registration errors were then compared between the 2 groups and within group E. The second part of this study was designed as a preliminary clinical study and was performed in 18 patients. Screening was performed to determine the combination of points on the body surface that provided the highest sensitivity to respiratory motion. Registration was performed either with (group E) or without (group C) the respiratory monitoring module. Registration errors were compared between the 2 groups. **Results:** In part 1 of this study, there were fewer registration errors at each point in group E than at the corresponding points in group C ($P < .01$). In group E, there were more registration errors at points A1 and B1 than at the other points ($P < .05$). There was no significant difference in registration errors among the remaining points. During part 2 of the study, there was a significant difference in the registration errors between the 2 groups ($P < .01$). **Conclusions:** Real-time fusion registration is feasible and can be accurately performed during respiratory motions when using this system.

Keywords

multimodal imaging, real-time image fusion, respiratory motion, liver neoplasms, ablation

Abbreviations

CT, computed tomography; DICOM, digital imaging and communications in medicine; MIF, multimodal image fusion; MRI, magnetic resonance imaging; RE, registration error; RPM, real-time position management; PTC, percutaneous transhepatic cholangiography; US, ultrasound

Received: January 02, 2018; Revised: April 04, 2019; Accepted: April 11, 2019.

Introduction

Over the past 2 decades, percutaneous thermal ablation has gained acceptance as an alternative method for treating liver tumors, particularly for small hepatocellular carcinoma.¹ A suitable image-guided approach is the basis of and a precondition for precise ablation. Current image guidance

¹ Department of Interventional Ultrasound, Chinese PLA General Hospital, Beijing, China

² Peking University Third Hospital, Beijing, China

³ Baihui Weikang Medical Robot Technology Co, Ltd, Beijing, China

Corresponding Author:

Ping Liang, MD, Department of Interventional Ultrasound, Chinese PLA General Hospital, 28 Fuxing Road, Beijing 100853, China.
 Email: liangping301@hotmail.com



technologies include ultrasound (US), computed tomography (CT), and magnetic resonance imaging (MRI). However, each imaging method has its own merits and flaws. Determining how to optimize imaging techniques and how they can complement each other to guide more precise ablation more precisely are key problems that need to be solved.

Multimodal image fusion (MIF) combines the advantages of multiple imaging technologies and provides important advantages for guided navigation.^{2,3} When using MIF, the target lesion is more clearly displayed, and this helps the operator to better grasp the spatial relationships between the tumor and surrounding tissues, thus permitting a more accurate tumor ablation surgery. Currently, MIF is used more in orthopedics and neurosurgery because of the relatively clear delineation and relative rigidity of the areas affected in their procedures.⁴⁻⁶ However, for abdominal tumors, such as those in the liver, movement caused by respiration makes the registration process more difficult.⁷ At present, the main method used to reduce registration errors (REs) caused by respiratory motion is artificial breathing cooperation.⁸ However, this does not sufficiently reduce REs. Several prediction methods have been established to accurately visualize liver deformations, but performing these methods is cumbersome and time-consuming.⁹⁻¹³ The purpose of this study was to establish a new fusion imaging system for real-time tumor tracking during respiratory motion and to validate the accuracy of registration during a specific breathing phase while using this system during ablation surgery.

Design of the OBERON System for Tumor Tracking With Respiratory Motion

The OBERON system is an image-guided surgery navigation system designed by our team and Tsinghua National Laboratory for Information Science and Technology. The system consists of a third-party US device coupled with an Aurora System via a magnetic sensor. The system is calibrated with the necessary parameters. Under a magnetic field, the US probe is registered to obtain 2-dimensional (2-D) US images in a 3-D space. Computed tomography images can also be used to position the tumor in 3-D space. Using these data, we can obtain a US-CT fusion image. When we use US for real-time scanning, the US-CT fusion image is presented.

Here, we provide an overview of the method. (1) By registering the US probe, the points in the 2-D US plane are mapped onto 3-D space, allowing us to obtain the 3-D coordinates of the target point in the US image. (2) A random forest model is applied under respiratory movement conditions to model the 3-D coordinates of body surface features and the target points in the body and to verify their accuracy. Based on this model, the coordinates of the target point in the body can be predicted from body surface features without using any imaging equipment. The ultimate goal is to achieve an accurate estimation of a position within the body from the body surface. The 2-D US images can be directly mapped onto a 3-D magnetic coordinate system, which can be transformed and registered with CT

image coordinates via a linear algebra transformation matrix method. The positions and attitudes of sensors placed on the abdominal surface can be obtained using real-time tracking of respiratory motions. The positions and attitudes of the sensors can then be converted to real-time errors using a mathematical algorithm. This provides a respiratory phase that is as similar as possible to that obtained in the preregistration CT images. The integrated algorithm used in this system was described in detail in our previous study.¹⁴

Compared to Varian real-time position management (RPM) and optical imaging equipment, this system provides the following advantages. (1) Varian RPM obtains only a limited number of individual positions (usually 1), whereas the system used in this study can simultaneously acquire the positions and orientations of up to 8 individual points, thus providing a more comprehensive analysis of surface features relative to respiratory movements. (2) Magnetic navigation provides a larger working space. Varian RPM and optical devices are both disadvantages in that they provide no shielding between the light source and the target, thus making it difficult for the doctor to perform surgery.

Materials and Methods

Instruments and Equipment

An electromagnetic tracking system (Aurora, NDI Medical, Canada) that included a field generator, sensors, sensor interface units, and a system control unit was used as the tracking system. A self-designed operation table equipped with an electromagnetic field generator was used as the examination bed for fusion registration. The table was not magnetically sensitive, and the electromagnetic field could therefore pass through it undisturbed. An ultrasonic diagnostic system (Sonix MDP, HOKAI Medical Equipment Co, Ltd, ZhuHai, China) was used to integrate the tracking system. A self-designed external marker layout containing 4 small steel balls could automatically be identified by the system and was used to acquire 3-D magnetic coordinates (Figure 1). A dual-source CT system (Siemens Medical Solutions, Forchheim, Germany) was used to obtain preprocedure CT images, and 21-gauge percutaneous transhepatic cholangiography (PTC) needles (Hakko, Tokyo, Japan) were used as puncture needles. Iodized oil (IPO, Guerbet, France) was injected into the livers of miniature pigs to simulate a focal liver lesion. A positioning bag (CaoYang Medical supplies factory, Shanghai, China) was used to ensure that the same body position was achieved when fusion registration was performed during the pre-CT examination. An air pump (YangYi Electrical Co, Ltd, China) was used to evacuate the air inside the positioning bag.

Part I: Animal Studies

Four male and female Guangxi Bama miniature pigs (weight, 15-20 kg) were selected. The Animal Ethics Committee of Chinese People's Liberation Army General Hospital approved

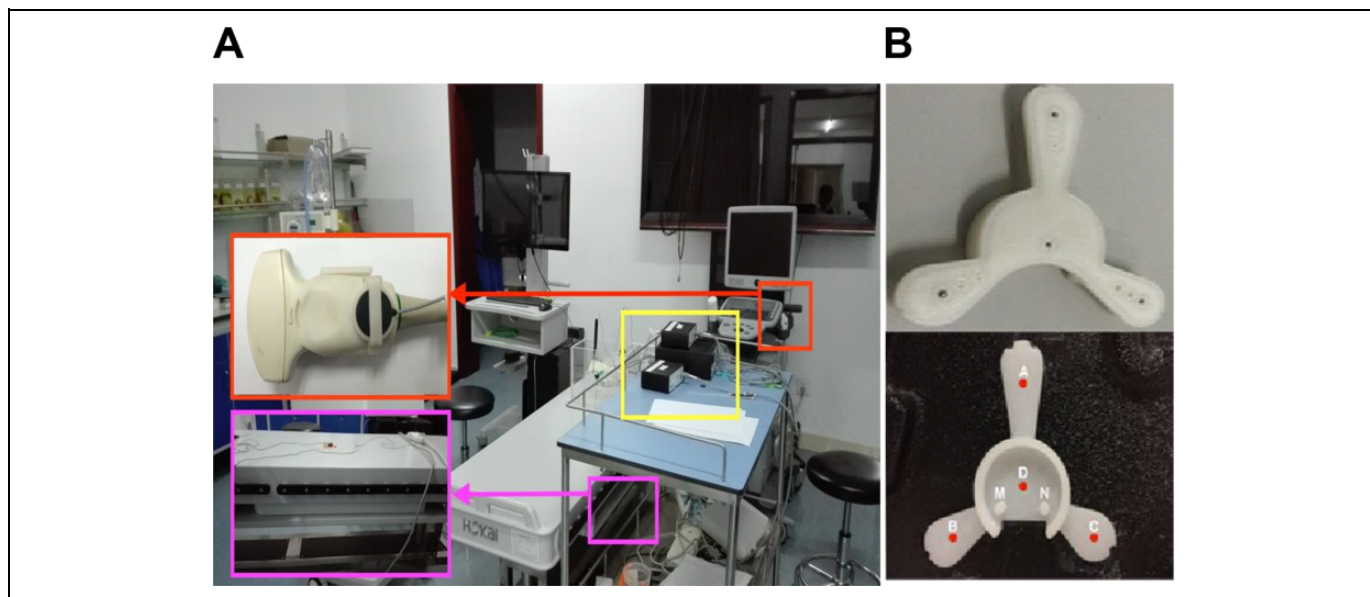


Figure 1. Main devices. A, The red rectangle shows the third-party US probe attached to a magnetic sensor. The pink rectangle shows the electromagnetic field generator embedded in the self-designed operation table. All magnetic sensors should be connected to system control unit shown in the yellow rectangle. B, The front and back views of the self-designed external marker layout. The image above shows 4 small steel balls inside the marker layout that can automatically be identified by the system. The image below shows the back view of the layout. Points A, B, C, and D correspond to the position of the 4 steel balls mentioned above. Points M, D, and N correspond to the position of the fixed magnetic sensor. US indicates ultrasound.

the experimental procedures (approval no. 2015-D11-06). All animal housing and experiments were conducted in strict accordance with the institutional Guidelines for Care and Use of Laboratory Animals.

Preparation of target points. Because iodized oil can be imaged with CT and US, orthotopic liver tumor models were established by injecting iodized oil into the livers of miniature pigs. In accordance with the relevant literature regarding the approach to registering respiratory motion in porcine livers *in vivo*,¹⁵ 4 representative points with 2 different sizes were selected as the registration target points (Figure 2). Combined, these points formed 8 target points that were expressed as A1-A4 and B1-B4 (Table 1). While the animals were under endotracheal general anesthesia, real-time US guidance was used to slowly and evenly inject the iodized oil into the liver via a 21-gauge PTC needle, resulting in a round sphere within the local liver parenchyma.

Preparation before CT scan. In general, CT examination tables are designed with a concave shape for the sake of patient safety. However, our self-designed operation table was flat and horizontal. This may have led to REs when the CT and US images were fused. Hence, in this study, a positioning bag was first placed in the area where the experimental pig would be scanned. The positioning bag was evenly smooth, and the air inside the bag was removed via an air pump. This setup achieved results equivalent to those obtained when using a horizontal CT examination table. The pig was fixed in a supine

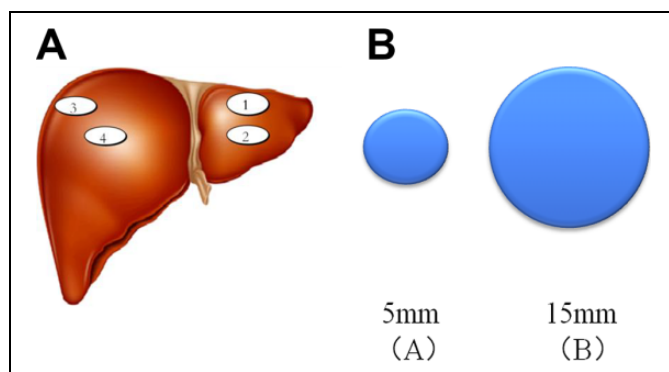


Figure 2. Diagram illustrating the selection of target points in the pig liver. A, Four different 520 locations were selected: near the surface of the left lateral lobe (1), inside the left lateral lobe (2), near the surface of the right lateral lobe (3), and inside the right lateral lobe (4) of the liver. B, The 2 different sizes, diameters of 5 and 15 mm, that were used at points A and B, respectively.

position or on the left side depending on the requirements of the scan.

Registration procedure. The exit of the endotracheal intubation tube inserted into the experimental pig was sealed during a specific breathing phase to maintain that specific breathing phase. A CT scan was then performed to acquire original data in digital imaging and communications in medicine (DICOM) format. The pig and the positioning bag were moved together to the operation table to avoid any error caused by a change in the pig's relative position during the transport process. Magnetic

Table 1. Sizes and Distributions of 8 Target Points.^a

A1	A2	A3	A4
Near the surface of the left lateral lobe of the liver $D = 0.5$	Inside the left lateral lobe $D = 0.5$	Near the surface of the right lateral lobe of the liver $D = 0.5$	Inside the right lateral lobe $D = 0.5$
B1	B2	B3	B4
Near the surface of the left lateral lobe of the liver $D = 1.5$	Inside the left lateral lobe $D = 1.5$	Near the surface of the right lateral lobe of the liver $D = 1.5$	Inside the right lateral lobe $D = 1.5$

^a“ D ” represents diameter (cm).

sensors were attached to the self-designed external marker and the third-party US probe. Then, the Aurora electromagnetic tracking systems was activated, and the OBERON system was initialized. In US FUSION mode, CT data were imported in DICOM format, and the results showed that this approach achieved a satisfying fusion of the registrations acquired by CT and US imaging. Registration was carried out at various points both with (experimental group E) and without (control group C) the respiratory monitoring module. In group E, during real-time aspiration error monitoring, the minimum respiration error for a certain breathing phase was defined as equivalent to that acquired during the breathing phase on a CT scan. The US-CT fusion registration procedure was performed in this specific breathing phase. In group C, the registration procedure was carried out during any breathing phase and without real-time respiration monitoring. In both groups, these registration procedures were performed 40 times for each target point. The REs were estimated by quantitative US measurement. The REs were then compared between the 2 groups and at each point in group E.

Part II: Preliminary Clinical Studies

Patient database. Eighteen male patients with liver tumors were enrolled (mean age, 56.8 years old). The tumors were located in the right lobe (12 cases) and the left lobe (6 cases). The tumor diameters ranged from 2.1 to 4.1 cm (mean, 3 cm).

Inclusion and exclusion criteria. The enrolled patients were required to meet the following criteria: (1) male ≤ 60 years old, (2) benign or malignant liver tumors with a maximum diameter ≤ 5 cm, (3) moderate stature with a body mass index ≤ 28 , (4) no ascites, (5) the ability to cooperate with instructions to change respiration and body position, and (6) no CT scan contraindications, such as a white blood cell count $\geq 4 \times 10^9/L$. Additional exclusion criteria included the following: a tumor that was not clear on CT and US imaging, a tumor with an extremely irregular shape, and the presence of refractory ascites or consolidation with severe respiratory and cardiovascular disease. Because of the noninvasive procedure, the ethical number was not required in this part. All patients provided written informed consent prior to enrollment in the study.

Selection of the points most sensitive to respiratory motions. Pilot experiments were performed to select the combination of positions that most accurately reflected respiratory motions on the body surface. Patients were placed in the left lateral decubitus position, and 8 sensors were attached to different positions on the body surface. The real-time positions of and pose changes associated with these 8 sensors were recorded (Figure 3A and B). To obtain the best and most stable respiratory monitoring information available with the minimal number of sensors, a combination of 3 of these 8 points was selected (providing 56 possible combinations). We then chose the combination that covered the largest relative proportion of positions and orientation changes and showed the best periodicity in the optimal configuration combination (ie, the mark of the actual position to be used for external marker layout; Figure 3C). Ultimately, in the left lateral decubitus position, the optimal combination of positions was determined to include the following: the periumbilicus, the intersection of the right anterior axillary line and costal margin, and the intersection of the horizontal line of the right posterior axillary line and the xiphoid. Similarly, in the supine position, the optimal combination of positions was determined to be the following: the periumbilicus and the intersection of the horizontal line of the left anterior axillary line and the xiphoid.

Registration procedure. The patient was placed in the left decubitus (12 cases) or supine (6 cases) position depending on the requirements of the ablation procedure. The patient’s position was fixed using a positioning bag, and a marker layout was placed on the patient’s body surface in the optimal combination of points that was previously determined to most sensitively reflect breathing motions (Figure 4A). A CT scan was performed during calm respiration, and original data in DICOM format were copied to a disk. The patient was moved to the operation table and asked to lie on the fixed positioning bag with the intent of making their position as consistent as possible with that used for the preoperative CT scan (Figure 4B). Two or 3 sensors were located on the marker layout on the patient’s body surface, as appropriate. A third-party US probe attached to a magnetic sensor was prepared. Then, the Aurora electromagnetic tracking system was activated, and the OBERON

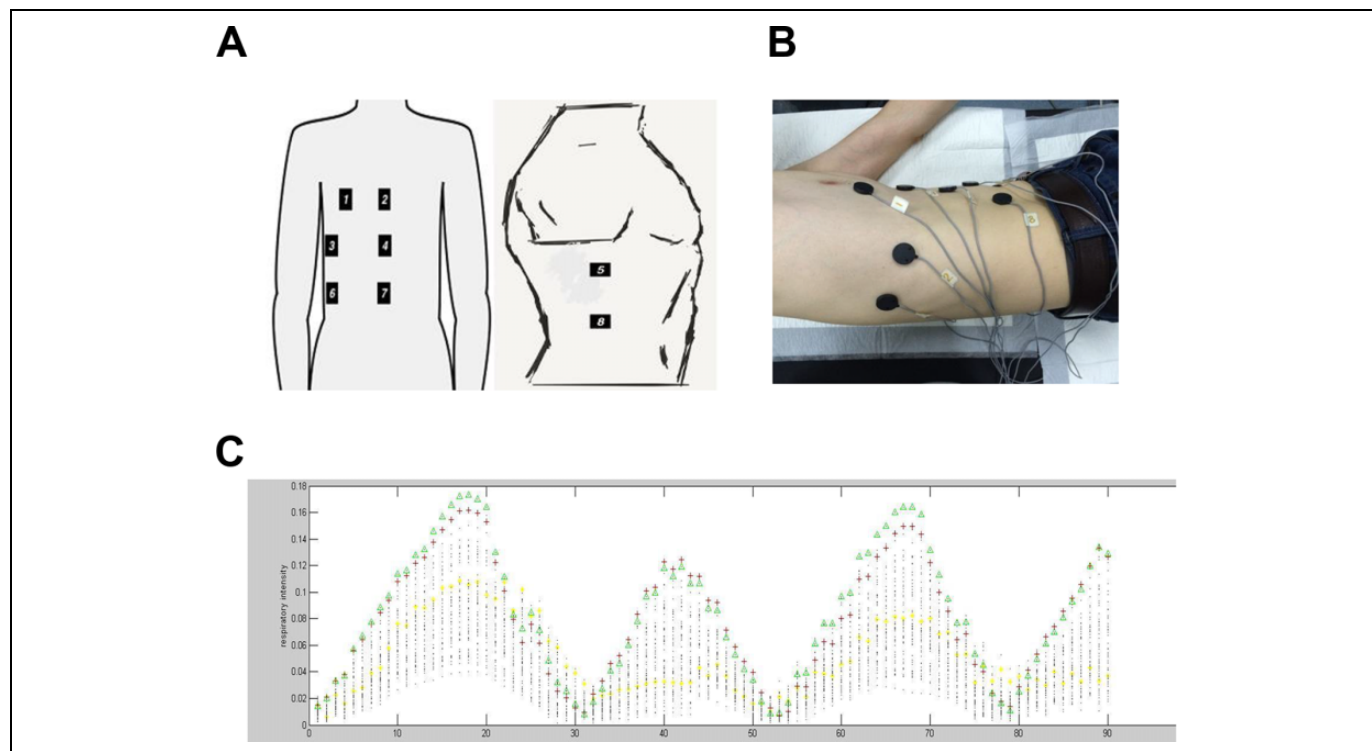


Figure 3. The pilot experiment used to select the combination of positions that most sensitively reflects respiratory motions. A, A diagram illustrating the positions of the 8 sensors on the body surface. B, The positions of the 8 sensors on the body of a human volunteer. C, The y -axis indicates the changes in the position of the 3 sensors relative to the initial position during respiration. The x -axis indicates the serial number of the sample collected. Each serial number on the x -axis corresponds to 56 points on the y -axis (arrangement combination:). All combinations of 3 out of the 8 sensors on the body surface were used to record breathing intensity, and we chose the combination of sensor positions that most sensitively reflected respiratory motion.

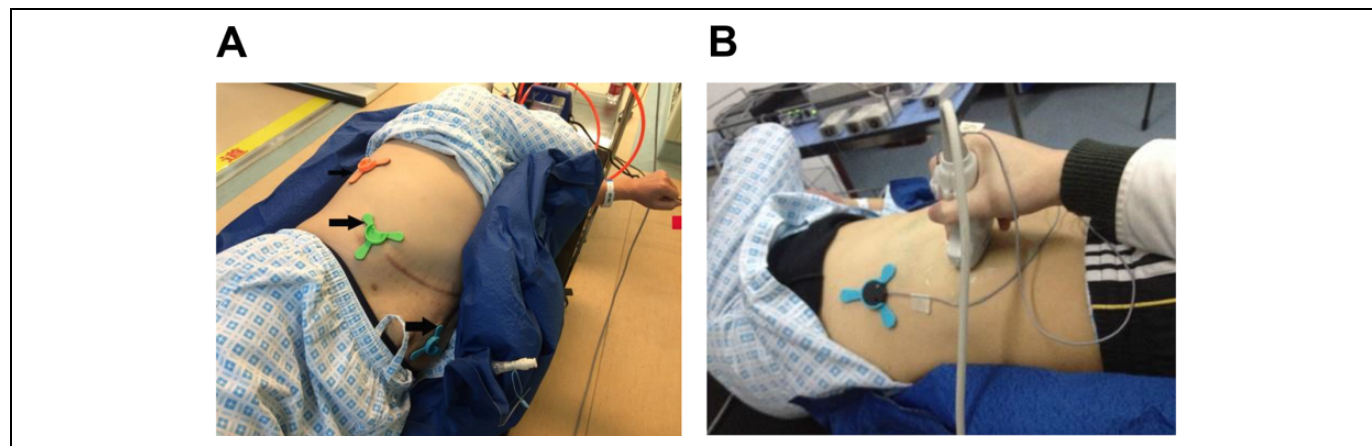


Figure 4. Preparation before the registration procedure on a patient with a liver nodule. A, The patient was fixed in place using a positioning bag, and the 3 marker layout was fixed on the patient's body at the optimal combination of points that was previously determined to most sensitively reflect breathing motion. B, A scan was performed with an ultrasonic transducer attached to sensors to acquire the 3-D magnetic coordinates.

system was initialized. While in the US FUSION mode, CT data in DICOM format were imported to achieve fusion registration. The registration was carried out either with (group E) or without (group C) the respiratory monitoring module. In group E, registration was performed when the error indicated by a real-time breathing motion error curve was minimal because

we considered that specific moment to be the time when the relative position and pose of the sensors placed on the patient's body were the same as those used during the previous CT scan. The patient was asked to hold their breath at this moment, and the registration procedure was performed to target the tumor. In group C, registration was carried out with the patient holding

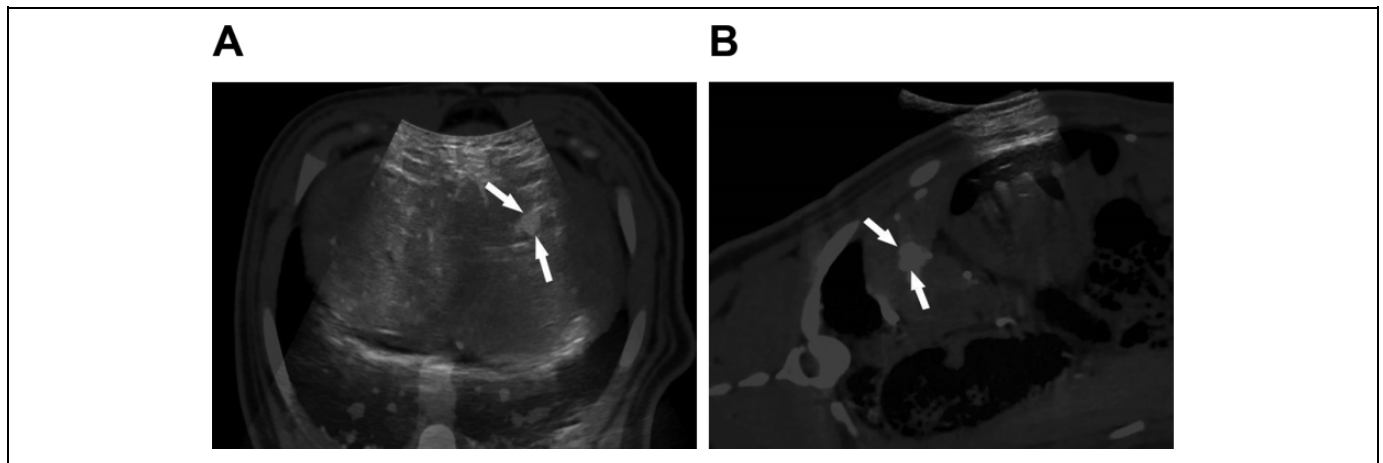


Figure 5. Picture of the registration of target points in the pig liver. A, Registration of a target point in the left lobe (arrow). B, Registration of a target point in the right lobe (arrow).

Table 2. Registration Errors for Each Point in the Pig Liver in the Experimental and Control Groups.^a

	A1	A2	A3	A4	B1	B2	B3	B4
E ₁	3.81 (0.24)	3.43 (0.37)	3.6 (0.36)	3.61 (0.41)	3.75 (0.32)	3.51 (0.37)	3.54 (0.36)	3.38 (0.47)
E ₂	4.45 (0.75)	4.41 (0.52)	4.43 (0.50)	4.59 (0.47)	4.52 (0.53)	4.35 (0.44)	4.33 (0.52)	4.4 (0.5)

^a“E₁” indicates the registration error in the experimental group (mm), while “E₂” indicates the registration error in the control group (mm).

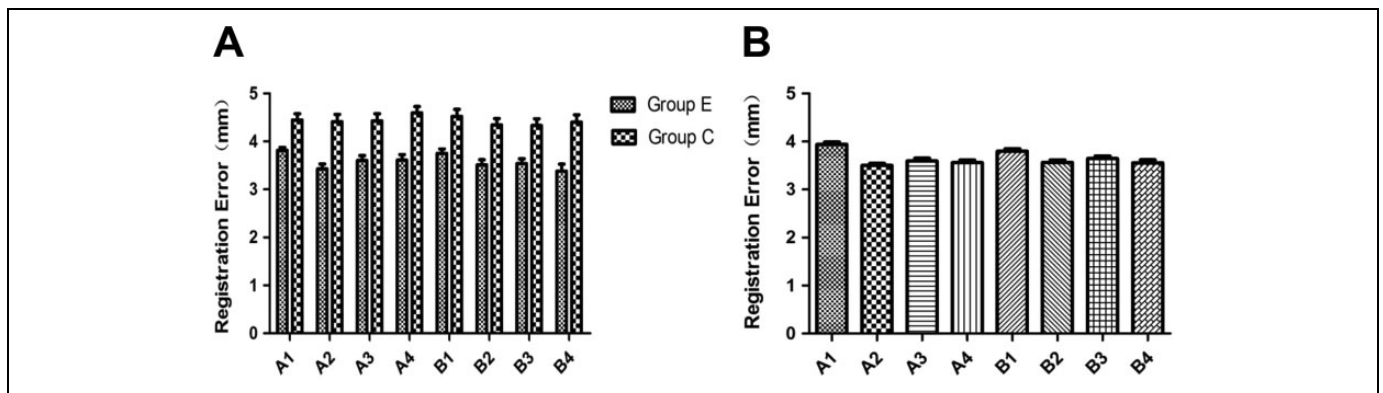


Figure 6. The registration errors (REs) of the 8 target points in the pig liver. A, The difference between groups E and C at each point. The RE was lower for each point in group E than in group C ($P < .01$). B, The REs for each point were compared in group E. The REs for points A1 and B1 (near the surface of the left lateral lobe of the liver) were higher than the REs at the rest of the points ($P < .01$). The REs were equivalent between A1 and B1 ($P > .05$). The REs were also equivalent among the remaining points ($P > .05$). Note: “Group E” represents the experimental group; “group C” represents the control group.

their breath at the end of inspiration. The REs of the 2 groups were measured and recorded.

Statistical analysis. Registration errors are presented as the mean (standard deviation). Normality and homogeneity of variance tests were performed on the data. Parametric tests were applied when normality (and homogeneity of variance) assumptions were satisfied. Otherwise, the equivalent nonparametric test was used. The data were analyzed using SPSS Statistics software (version 17.0). P values $< .05$ were considered statistically significant.

Results

Animal Study

The registration procedure was successfully performed at all points (Figure 5). The RE of each point was lower in group E than that in group C (Table 2). There was a significant difference between the 2 groups ($P < .01$; Figure 6A).

When REs were compared between each pair of points in group E, the REs were larger for points A1 and B1 (near the surface of the left lateral lobe of the liver) than for the rest of

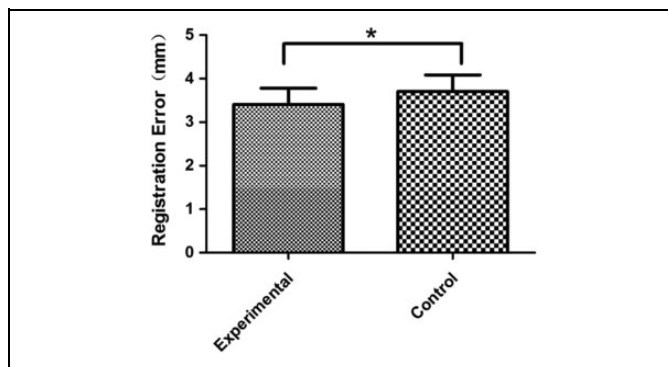


Figure 7. The registration errors (Res) were compared between the 2 groups. Note that the RE was significantly lower in group E than in group C ($P < .05$).

the points. The REs of these 2 points were significantly different than those for other points, but REs was not significantly different between A1 and B1 ($P > .05$). The REs among the remaining points were not significantly different ($P > .05$; Figure 6B).

Clinical Study

The optimal combination of positions was selected to reflect the respiratory motions of the patients with sufficient sensitivity. The registration procedure was successfully achieved in 18 patients. The RE was significantly lower in group E (3.41 [0.39] mm) than in group C (3.71 [0.34] mm; Figure 7).

Discussion

Precise imaging guidance is key to achieving a successful liver tumor ablation. This approach guarantees a reasonable needle distribution within the tumor and the establishment of an effective thermal field as well as ensuring that no injury occurs in important surrounding structures, such as the diaphragm, gastrointestinal tract, bile duct, and large vessels.¹⁶⁻¹⁹ Wright²⁰ equated the importance of imaging with that of the eyes of the surgeons, indicating that image guidance plays a decisive role in the treatment process. In recent years, to overcome the shortcomings associated with performing procedures using a single image, MIF technology has gradually been applied in the field of tumor ablation.^{21,22} However, the liver is substantially deformed and displaced by respiratory movements. Indeed, the liver can be displaced by an average craniocaudal distance of as much as 10 to 40 mm during normal respiration and 30 to 80 to 260 mm during deep respiration,²³ and this can lead to a higher RE and a greater chance of damaging the surrounding tissue.²⁴

Currently, the main method used to reduce the RE caused by respiratory motion is artificial breathing cooperation.⁸ The specific approach is as follows: First, the section being visualized with the US probe is kept consistent with the section imaged on CT/MRI. Second, while the patient holds their breath, the registration procedure is carried out relative to certain feature points, such as a vascular bifurcation, cyst, or calcification.

Then, the initial registration is completed. If the registration accuracy is satisfactory, intraoperative navigation can be initiated. If the accuracy is not sufficient, the second step is repeated until satisfactory registration accuracy is achieved. It is generally necessary to repeat the second step 2 to 3 times. However, when the method described above is used for registration, the data obtained during the respiratory phase are likely to be different from the data obtained on the preoperative CT scan, resulting in REs. Although REs caused by the respiratory phase can, to a certain extent, be adjusted for, this approach takes time. In addition, during the procedure, the patient needs to hold their breath multiple times. The breathing phase imaged during each of these breath-holding cycles may be different from the breathing phase used for registration. Hence, actual error can only be controlled within a relatively small range and cannot be reduced to a desired minimum.

Various prediction methods have been established to estimate liver deformation. Linear predictive models^{9,10} are used to estimate the future tumor position based on the linear accumulation of external signals. Because the curve for respiratory motion is nonlinear, the Kalman filter was adapted to introduce weak nonlinearity into the predictive model.¹¹ However, its heavy computational load and weak linearity limit its further application. Artificial neural networks have also substantially advanced predictive performance despite the fact that they require time-consuming computations.^{12,13} Our group has proposed a simple 3-D navigation strategy, and we have designed a fast tumor tracking system to handle respiratory motion.¹⁴ The elaborate system we designed for navigation was based on a method that combines rigid registration transformation and real-time respiratory-phase monitoring. It can fuse registrations obtained in intraoperative multimodal images and real-time navigation under conditions involving respiratory motion. This may make the target lesion more visible and reduce the incidence of injury to surrounding normal tissues.

Our results show that the OBERON system, a real-time monitoring module, reduced REs at different liver locations and maintained accuracy at a more satisfactory level than was achieved using a conventional approach. In an animal study, the REs were higher at points A1 and B1 than at the rest of the data points ($P < .01$). One possible reason for this difference is that the liver is more substantially deformed at the surface of the left lateral lobe than at other sites. This could be because there is more squeezing pressure from the diaphragm and other organs in the vicinity or increased pressure from the US probe due to a reduced gas interference. The lack of ribs or protection by other skeletal system components could also be a contributing factor. The REs at points A3 and B3 were not significantly different from those at the other points except for A1 and B1, but the average value of the 2 points was higher. This difference could be due to the presence of a minor liver deformation near the surface of the right lateral lobe, which is protected by the ribs. The other sites located inside the liver (points A2, B2, A4, and B4) are less affected by external forces and had lower REs.

We also found that the REs in our clinical study were lower than those we observed in our experimental study. There are some possible reasons for this difference. (1) Position factors may have contributed, in that patient cooperation was better when the patient maintained a consistent position during both the preoperative CT scan and the registration procedure. However, in the experimental pigs, the position may have changed during the procedure and could not be consciously adjusted. (2) The sensitivity of respiratory motion monitoring may also have affected results in the human study: Before performing the fusion registration procedure, a screening experiment was conducted to optimize marker position selection on the body surface. In the clinical study, we performed an analysis to determine the optimal combination of points on the body surface that most sensitively reflected respiratory motion error.

The respiratory movements of the liver are complex and an important factor that contributed to error during the registration process with MIF. In this study, some measures were taken to reduce the interference caused by other factors, as follows: (1) We used a positioning bag to attempt to ensure that the same body position and pose that were achieved during the preoperative CT examination were also achieved when performing the fusion registration; (2) we maintained a specific breathing phase in the pigs by blocking the established artificial airway for a short time during breath module monitoring, and this allowed us to maintain the pigs in the same relative position and pose; (3) in the clinical study, we chose only male patients as research participants to eliminate differences in the displacement of the abdominal organs that can be caused by differences in breathing methods between men and women (eg, men more frequently use belly breathing, while women more frequently use thoracic breathing); (4) we selected the combination of positions on the body surface that we found most sensitively reflected respiratory motion to obtain accurate rules for respiratory motion; and (5) we placed the patient's body into the left lateral or supine position during the preregistration CT baseline scan because it is commonly used during US-guided ablation in order to minimize RE caused by body position.

Despite the encouraging results presented here, there is much room for improvement. First, this is only a preliminary study, and the number of tested patients may be insufficient. Hence, further experiments should be designed to include more patients. Second, the system is experimental and not perfect, because the program getting more and more computationally inefficient due to memory or CPU management issues. We believe that as the software is upgraded, the issue will be resolved. In the future, the time for which the results obtained by our method are valid should be tested to ensure that surgeries proceed safely and smoothly. Third, the elaborately designed external marker layout used in this study can only be identified by CT and is not compatible with MRI. Moreover, the large size of the external markers may lead to patient discomfort. More marker features should, therefore, be tested to further optimize the system. Finally, various factors may affect the accuracy of fusion registration. Although we attempt to control for some interfering factors, some objective factors could not

be completely avoided. For instance, the degree of liver deformation cannot be artificially controlled, and the position of the body will never be exactly the same when a patient or animal is transferred from the CT examination bed to the customized operation table. How we might properly match the magnetic field generator to the CT examination bed to allow CT scanning and registration work to be performed in the same location is a problem that remains to be solved.

Conclusions

The OBERON system can record real-time respiratory motion and provide the respiratory phase error created in the liver by respiratory motility factors. The RE caused by respiratory motion can, to some extent, be reduced by controlling for the breathing phase. However, because the respiratory movements performed in the human body are complex and variable, accurately tracking respiratory motions and accurately achieving registration across different circumstances (such as the tumor location, size, and nature) in liver neoplasms require further clinical study.

Authors' Note

Chao Ren and Shi-rong Liu contributed equally to the manuscript. The authors alone are responsible for the content and writing of the article.


Declaration of Conflicting Interests

The author(s) declared no potential conflicts of interest with respect to the research, authorship, and/or publication of this article.

Funding

The author(s) disclosed receipt of the following financial support for the research, authorship, and/or publication of this article: This study was supported by the National Key R&D Program of China (2017YFC0112000) and by the National Natural Science Foundation of China (grant numbers 81627803, 81401436, and 81622024).

ORCID iD

Chao Ren, MD  <https://orcid.org/0000-0001-9302-5888>

References

1. Tombesi P, Di Vece F, Sartori S. Resection vs thermal ablation of small hepatocellular carcinoma: what's the first choice? *World J Radiol.* 2013;5(1):1-4.
2. Geevarghese R, O'Gorman Tuura R, Lumsden DE, Samuel M, Ashkan K. Registration accuracy of CT/MRI fusion for localisation of deep brain stimulation electrode position: an imaging study and systematic review. *Stereotact Funct Neurosurg.* 2016; 94(3):159-163.
3. Paparo F, Piccazzo R, Cevasco L, et al. Advantages of percutaneous abdominal biopsy under PET-CT/ultrasound fusion imaging guidance: a pictorial essay. *Abdom Imaging.* 2014;39(5): 1102-1113.
4. Pirris SM, Nottmeier EW. A case series on the technical use of three-dimensional image guidance in subaxial anterior cervical surgery. *Int J Med Robot.* 2015;11(1):44-51.

5. Härtl R, Lam KS, Wang J, Korge A, Kandziora F, Audigé L. Worldwide survey on the use of navigation in spine surgery. *World Neurosurg.* 2013;79(1):162-172.
6. Jang SH, Cho JY, Choi WC. Novel method for setting up 3D navigation system with skin-fixed dynamic reference frame in anterior cervical surgery. *Comput Aided Surg.* 2015;20(1):24-28.
7. Feuerstein M, Reichl T, Vogel J, Traub J, Navab N. New approaches to online estimation of electromagnetic tracking errors for laparoscopic ultrasonography. *Comput Aided Surg.* 2008;13(5):311-323.
8. Woodford C, Yartsev S, Van Dyk J. Image registration of a moving target phantom with helical tomotherapy: effect of the CT acquisition technique and action level proposal. *Phys Med Biol.* 2008;53(18):5093-5106.
9. Sharp GC, Jiang SB, Shimizu S, Shirato H. Prediction of respiratory tumour motion for real-time image-guided radiotherapy. *Phys Med Biol.* 2004;49(3):425-440.
10. Verma PS, Wu H, Langer MP, Das IJ, Sandison G. Survey: real-time tumor motion prediction for image-guided radiation treatment. *Comput Sci Eng.* 2011;13(5):24-35.
11. Lee SJ, Motai Y, Murphy M. Respiratory motion estimation with hybrid implementation of extended Kalman filter. *IEEE Trans Ind Electron.* 2012;59(11):4421-4432.
12. Murphy MJ, Pokhrel D. Optimization of an adaptive neural network to predict breathing. *Med Phys.* 2009;36(1):40-47.
13. Park S, Lee SJ, Weiss E, Motai Y. Intra- and interfractional variation prediction of lung tumors using fuzzy deep learning. *IEEE J Transl Eng Health Med.* 2016;4:1-12.
14. Tian Q, Song Y, Ren C. Real-time tumor tracking with respiratory motion based on short-term prediction. In: *2nd International Conference on Control, Automation and Artificial Intelligence (CAAI 2017)*, 2017, pp. 499-503.
15. Srimathveeravalli G, Leger J, Ezell P, Maybody M, Gutta N, Solomon SB. A study of porcine liver motion during respiration for improving targeting in image-guided needleplacements. *Int J Comput Assist Radiol Surg.* 2013;8(1):15-27.
16. Bourquain H, Schenk A, Link F, Preim B, Prause G, Peitgen HO. Hepavision2: a software assistant for preoperative planning in living-related liver transplantation and oncologic liver surgery. In: *Computer Assisted Radiology and Surgery: Proceedings of the 16th International Congress and Exhibition*, Paris, 26–29 June 2002, pp. 341-346.
17. Delingette H, Ayache N. Hepatic surgery simulation. *Commun ACM.* 2005;48(2):31-36.
18. Hansen C, Köhn A, Schlichting S, et al. Intraoperative modification of resection plans for liver surgery. *Int J Comput Assist Radiol Surg.* 2008;3:291-297.
19. Schwier M, Dicken V, Peitgen H. 3D visualization of vascular structures around liver tumors using fuzzy clustering. In: *International Congress and Exhibition "Computer Assisted Radiology and Surgery" (CARS)*, Barcelona, 2008, pp. 403-404.
20. Wright J. Surgery: the eyes of the operation. *Nature.* 2013; 502(7473):S88-S89.
21. Lee MW, Rhim H, Cha DI, et al. Percutaneous radiofrequency ablation of hepatocellular carcinoma: fusion imaging guidance for management of lesions with poor conspicuity at conventional sonography. *AJR Am J Roentgenol.* 2012;198(6): 1438-1444.
22. Liu FY, Yu XL, Liang P, et al. Microwave ablation assisted by a real-time virtual navigation system for hepatocellular carcinoma undetectable by conventional ultrasonography. *Eur J Radiol.* 2012;81(7):1455-1459.
23. Suramo I, Päävänsalo M, Myllylä V. Cranio-caudal movements of the liver, pancreas and kidneys in respiration. *Acta Radiol Diagn (Stockh).* 1984;25(2):129-131.
24. Rosu M, Dawson LA, Balter JM, McShan DL, Lawrence TS, Ten Haken RK. Alterations in normal liver doses due to organ motion. *Int J Radiat Oncol Biol Phys.* 2003;57(5):1472-1479.